Mineralogical Magazine, October 2005, Vol. 69(5), pp. 897–906

Arsenic-bearing smectite from the geothermal environment

C. PASCUA[1], J. CHARNOCK[2,3], D. A. POLYA[3], T. SATO[4,*], S. YOKOYAMA[5] AND M. MINATO[1]

[1] Graduate School of Natural Science and Technology, Kanazawa University, Kanazawa, Ishikawa 9201192, Japan
[2] CCLRC Daresbury Laboratory, Daresbury, Warrington WA4 4AD, UK
[3] School of Earth, Atmospheric and Environmental Sciences & Williamson Research Centre for Environmental Science, The University of Manchester, Oxford Road, Manchester M13 9PL, UK
[4] Institute of Nature and Environmental Technology, Kanazawa University, Japan
[5] Ecomaterials Center, National Institute for Materials Science, Japan

ABSTRACT

Arsenic-rich scales are widely associated with geothermal fields and constitute a potential hazard to human health. Such arsenic has hitherto been reported to be almost exclusively hosted by sulphide or oxide phases or occurring as surface species. We report here, however, the occurrence of an arsenic-rich (1500 to 4000 mg kg^{-1} As) smectite from geothermal precipitates from a geothermal field in northwestern Japan and present evidence that the arsenic is predominantly hosted within this silicate mineral.

Consistently ~80% of the total arsenic determined in these geothermal precipitates was found by selective chemical extractions to be associated with an operationally defined clay mineral fraction, with lesser proportions being associated with operationally defined amorphous silica, Fe oxide and sulphide fractions. Analysis by XRD, ATR IR and XRF showed the clay fraction to be dominated by Mg-rich trioctahedral smectite.

Arsenic K-edge XAS spectra of the smectite suggested the dominance of As(III)-O coordinated species with significant contributions from As(V)-O coordinated species. Both XPS and a magnesium chloride chemical extraction indicated minimal adsorption of arsenic on smectite surfaces suggesting that the arsenic was predominantly either dissolved within the smectite or occurred within mineral occlusions. No such occlusions greater than 1 μm in size were observed in the As-rich smectites.

The potential occurrence of arsenic-bearing clays should be considered when determining remediation strategies for geothermal environments or evaluating risks associated with the industrial usage of geothermal precipitates.

KEYWORDS: arsenic, smectites, XAS, geothermal, Japan.

Introduction

PRODUCTION of energy from geothermal power plants might typically involve several decades of operation and the consequent accumulation of a large amount of geothermal precipitates. These precipitates normally contain trace amounts of arsenic and heavy metals (Peralta *et al*., 1996). Most of these geothermal precipitates are re-injected into the deep sub-surface in the form of a slurry; however there is considerable interest in the conversion of geothermal precipitates for industrial purposes, for example as a source of silica. It is therefore important to assess the risks arising from the release of trace components such as arsenic not only during temporary storage and consequent potential contamination of areas that surround the power plants, but also during and after any industrial conversion process.

Identification of possible mineralogical hosts of arsenic, which are ubiquitous in the geothermal environment, is important in assessing arsenic mobility and risks to human health (cf. Ellis, 1977; Smedley and Kinniburgh, 2002). Under reducing conditions, sulphide minerals commonly host arsenic in the geothermal environment (Criaud and Fouillac, 1989; Ballantyne and

* E-mail: tomsato@kenroku.kanazawa-u.ac.jp
DOI: 10.1180/0026461056950297

Moore, 1988) whilst under oxidizing conditions the surfaces of Fe-Mn oxyhydroxides, carbonates and clays are generally the arsenic sinks (Le Guern *et al*., 2003; Arnorsson, 2003).

In this study, the distribution of arsenic in geothermal precipitates from Japan has been determined. We use a combination of mineralogical techniques to demonstrate, we believe for the first time, that arsenic may be hosted within silicate phases within such geothermal precipitates.

Samples and methods

Samples and context

Four geothermal precipitates (labelled as B-2, C-6, CE-1 and E-9), also referred to here as geothermal scales due to their scale-like appearance inside pipelines, were collected from a geothermal field in Akita prefecture, northwestern Japan. These samples represent deposits removed from the pipelines during regular maintenance operations (i.e. every three years). The geothermal fields lie on the western edge of a north–south graben structure bounded by an east–west trending volcanic chain (Inoue and Ueda, 1965). It is underlain by Quaternary volcanic rocks, lacustrine sediments, and Tertiary formation (volcanic rocks and marine sediments) and was intruded by granitic rocks (Yora *et al*., 1973; Sakai *et al*., 1986; Okuma 1998). The geothermal fluids, prior to exploitation of the geothermal fields for electricity generation, have been described as near-neutral pH Na-Cl type geothermal fluids resulting from the mixture of deep Cl-rich water and shallow heated SO_4-HCO_3 rich water (Ueda *et al*., 1991). The SO_4 content of the original geothermal fluid originated primarily from the dissolution of anhydrite in the reservoir, and oxidation of H_2S. The Mg concentration is generally low and enrichment is due to the dissolution of Tertiary andesites resulting from the mixing of acidic fluids from other sources (Ueda *et al*., 1991). The geothermal fluid has a relatively small amount of total dissolved solids content compared to other geothermal systems in Japan (Ueda *et al*., 1991). The average geochemical composition of the geothermal fluid during geothermal energy exploitation has been determined by Kato *et al.* (2003) and is presented in Table 1. Preliminary *in situ* measurement of arsenite in the fluid by test kit (HIRONAKA BVC-W100) and calculation of arsenate by difference (Table 1) suggests that geothermal fluid arsenic speciation was dominated by As(III): this is typical of most similar geothermal environments (cf. Polya *et al.*, 2003). Other aspects of the geothermal field are described by Pritchett *et al.* (1989), Inoue *et al.* (1999), Ariki *et al.* (2000) and Kumagai *et al.* (2004).

Bulk mineralogical characterization

The scales were initially observed under an optical binocular microscope. Powder X-ray diffraction (XRD; Rigaku RINT-1200 with Cu-$K\alpha$ radiation) was used to detemine the major crystalline phases present. The geothermal scales were then pre-treated with 0.1 M NaOH for 24 h to remove excess silica prior to determination of major element composition by X-ray fluorescence spectrometry (XRF; Rigaku 3270 X-ray Spectrometer). Attenuated total reflection infrared (ATR-IR; Jasco FTIR-610V and Pike MIRacle) spectroscopy was also performed on bulk samples. Scanning electron microscopy (SEM; Jasco JSM-5600LV) imaging in conjunction with energy dispersive X-ray spectrometry (EDS; Oxford Microanalysis Group EDS Link Isis) was used for micro-chemical analyses.

Selective chemical extractions

Sequential selective chemical extractions were performed to assess the mineralogical distribution

TABLE 1. Typical composition (mg l^{-1}) of the geothermal fluid, after Kato *et al.* (2003) except for arsenic speciation determined in this study.

Parameter	Value
T	90ºC
pH	7.5
Total As	13
As (III)	10
As(V)	3
Al	1.4
Fe	0.04
Mg	0.5
Ca	8
K	64
Na	393
Total SiO_2	729
SO_4	159
H_2S(aq)	<0.1
Cl	572
Total CO_2	45

of arsenic in the geothermal scales. The two schemes, based in part on those published by Tessier *et al.* (1979) and Ianni *et al.* (2001), were employed and are outlined in Table 2.

Scheme A was aimed to extract arsenic from operationally defined surface (step 1), silica-complexed (step 2) and clay mineral (step 3) fractions. Exactly 1 g of finely powdered (<2 μm) sample was initially placed inside a polyethylene centrifuge tube. For the first step, a 0.3 M $MgCl_2$ solution adjusted to pH 8 was added and the tube was continuously shaken for 24 h. Then, the sample was centrifuged for 40 min at 3500 rpm in order to separate solids from liquids. The extract was filtered through a syringe-mounted 0.20 μm filter. The remaining solids were rinsed with additional $MgCl_2$ solution and centrifuged. The filtered rinsing solution was then added to the first extract. Extracts were stored in polyethylene bottles and refrigerated. The remaining solids were washed with distilled deionized water and centrifuged to separate the solid from the liquid. The water used for washing was discarded. The solids were then carried over to the next step. In the second step, 50 ml of 1 M NaOH were added to the solids and shaken for 24 h. The solids were rinsed with 10 ml of NaOH, shaken manually and then centrifuged. The filtered liquid was added to extracts and stored. The solids were washed with distilled, deionized water, shaken manually with occasional ultrasonification, centrifuged to separate solids and liquids, then the liquid discarded and the solids freeze-dried overnight. Exactly 100 mg of these solids were then carried over to the next step. For the third step, the solids carried over were reacted with 50 ml of concentrated nitric acid and 20 ml of concentrated hydrofluoric acid for several hours with occasional manual agitation. Concentrated extracts were diluted to 100 ml for analysis. Scheme B was performed to determine arsenic extractable from operationally defined oxide (reducible) (step 1), sulphide (step 2) and clay mineral (step 3) fractions. Exactly 1 g of finely ground sample (<2 μm) was initially placed inside a centrifuge tube. For the first step, a 1 M ammonium acetate solution adjusted to pH 4 with acetic acid was added and shaken continuously for 24 h. The solid and liquid were separated by centrifugation. Extracts were then filtered with syringe-mounted 0.2 μm filters. Solids were then rinsed with additional ammonium acetate solution. The rinsing solution was added to the extracts, acidified with nitric acid and refrigerated for storage until analysis. The remaining solids were washed with distilled, deionized water. The water used for washing was discarded. The solids were then mixed with a 1 M ammonium oxalate solution adjusted to pH 4 by oxalic acid and reacted with continuous shaking for 24 h at 80ºC using a water bath and whilst being kept in the dark by wrapping in aluminium foil. Similar filtering and washing procedures from the previous step were carried out. In the third step, concentrated hydrogen peroxide (37%) was added to the solids and shaken continuously for 24 h at room temperature. Analogous filtering and washing procedures from previous steps were carried out. After washing, the solids were freeze-dried and carried over to the next step. For the third step, only a small fraction of the sample from the previous step was utilized (100 mg). A mixture of three parts concentrated HNO_3 and two parts concentrated HCl (3:2 HNO_3-HCl) was used to extract arsenic from the remaining solids. The suspension was maintained at 80ºC in a water bath with intermittent manual shaking. The extract was separated from the solids by centrifugation and passed through syringe-mounted 0.2 μm filters.

Arsenic concentrations in extracts from steps 1 and 2 of scheme A were determined by inductively coupled plasma-mass spectrometry

TABLE 2. Summary of the sequential selective chemical extraction methods employed in this study, together with associated phases operationally defined by each extraction step.

Scheme A		Scheme B	
Reagent	Phases	Reagent	Phases
0.3 M $MgCl_2$ (at pH 8)	Surface sorbed	1 M NH_4-acetate + 1 M NH_4-oxalate (at pH 4)	Fe oxyhydroxide (reducible)s
1 M NaOH	Silica complexed	Conc. H_2O_2 (37%)	Sulphides
2:1 concentrated HNO_3 + HF	Clays	3:1 concentrated HNO_3 + HCl	Clays

(ICP-MS) at the Department of Chemistry, Kanazawa University; extracts from step 3 of scheme A were analysed at the National Institute for Materials Science (Tsukuba, Japan); whilst all extracts from scheme B were analysed in the ICP-MS facility of the Japan Atomic Energy Research Institute (Ibaraki, Japan). The selection of analytical facilities was dictated both by suitability and availability.

X-ray photoelectron spectroscopy (XPS)

Limited surface chemical analyses of the bulk samples using the XPS (Esca Absenta 300) facility of the Japan International Centre for Agricultural Research (Tsukuba, Japan) were performed to assess the accumulation of arsenic on mineral surfaces. Mineral phases present in concentrations too low to be identified by XRD may be inferred by this technique. Short-term scans (e.g. 1–9 h) were performed initially and later increased to 24 h scans to enhance the sensitivity.

Synchrotron-based X-ray spectroscopy

Synchrotron-based X-ray absorption spectroscopy (XAS) data were collected at the CLRC Daresbury Laboratory Synchrotron Radiation Source (SRS) on beamline station 16.5 following procedures described by Gault *et al.* (2003, 2005). The X-ray absorption neare-edge structure (XANES) was used to determine the dominant oxidation state of arsenic (i.e. As^{III} *vs*. As^{V}) in the solid phases by quantitative comparison with the XANES spectra of model arsenic compounds using *LINCOM* software (http://srs.dl.ac.uk/XRS/index.htm) (Rowland *et al.*, 2005). Arsenic K-edge extended X-ray absorption fine structure (EXAFS) spectra fitted according to methods outlined by Gault *et al.* (2003, 2005) provided insights into the local coordination environment of As. Two bulk samples were analysed, namely B-2 and C-6. Four scans of ~50 min duration each for both samples were collected. For each sample, these scans were combined to increase the signal to noise ratio.

Results

Mineralogy

The geothermal precipitates were found to be predominantly composed of fine-grained white, crystalline smectite and translucent amorphous silica with traces of oxide and sulphide minerals, the latter observed by optical microscopy to occur as occlusions within the amorphous silica. X-ray diffraction (Fig. 1) confirmed the predominance of smectite, a swelling clay mineral that can accommodate various ions in its interlayer spaces and substitutions in their sheet structures (see Velde, 1992 for a thorough discussion). Imaging by SEM (Fig. 2) revealed crystalline smectite grains cemented and coated with amorphous silica. No sulphide or oxide minerals

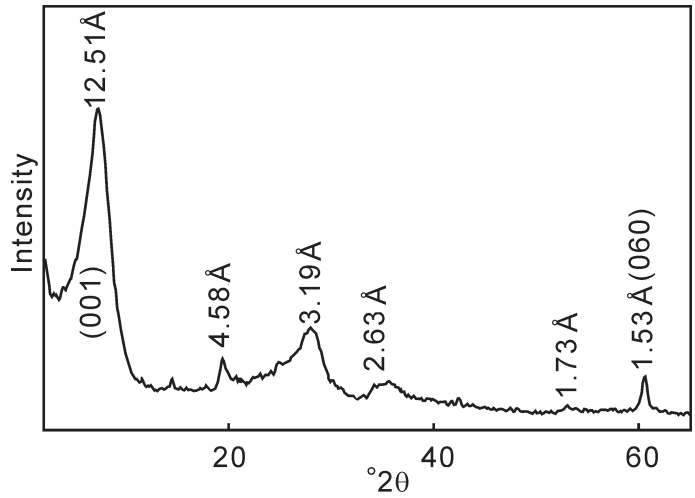

FIG. 1. A representative XRD pattern of a geothermal scale (C-6) composed primarily of a trioctahedral smectite. The diffraction peak at 1.53 Å is comparable to the 060 peak characteristic of trioctahedral smectites (Cu-*K*α radiation).

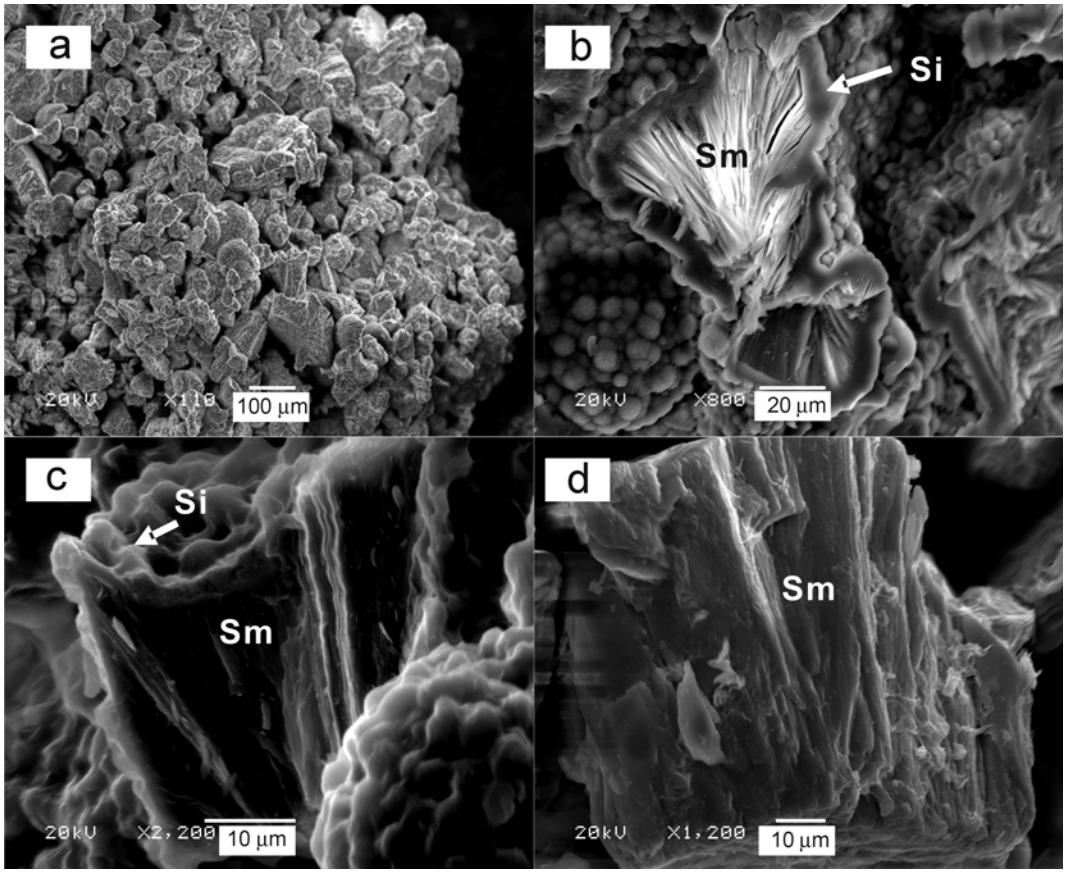

FIG. 2. SEM images showing (*a*) smectite particles comprising the geothermal scales cemented together by amorphous silica; (*b*) amorphous silica encapsulating a smectite particle; (*c*) stacked smectite laths coated with amorphous silica; and (*d*) stacked smectite laths without any such coating. Legend: Sm – smectite; Si – amorphous silica.

were detected by either by XRD of bulk samples or by qualitative SEM EDS chemical mapping of individual smectite grains or somewhat larger areas; these results confirm that these phases constitute only a minor fraction of the precipitates.

The smectites were determined to be trioctahedral type on the basis of the observation of a 060 diffraction peak at ~1.530 Å (cf. Velde, 1992). The XRF analysis (Table 3) and EDS microanalysis (data not shown) indicated the

TABLE 3. XRF chemical analyses of geothermal precipitates modified as detailed in the text. The high SiO_2 contents indicate that not all amorphous silica has been removed from these samples. All values expressed as wt.%.

Sample	SiO_2	TiO_2	Al_2O_3	Tot. Fe	MnO	MgO	CaO	Na_2O	K_2O
B-2	56	0.1	6.9	4.6	1.9	20	2.2	0.9	0.6
C-6	59	0.1	7.5	2.7	1.5	18	2.0	1.1	0.9
CE-1	59	0.1	7.6	2.4	1.4	17	2.0	1.1	0.9
E-9	61	0.1	8.3	2.5	1.4	16	2.0	1.2	1.0

smectites to be Mg-rich whilst IR spectra (data not shown) were closely similar to the those of stevensite, a Mg-rich trioctahedral smectite.

Arsenic distribution in the geothermal scales

The total arsenic concentration of the geothermal scales was determined by chemical extractions to range approximately from 2500 to 4600 mg kg^{-1} (Table 4). These results are broadly consistent with the qualitative SEM EDS determination of high arsenic concentrations in the smectite (5000 to 14000 mg kg^{-1}) and non-detectable arsenic concentrations in the amorphous silica coating or cement and suggest that the bulk of the arsenic in these scales is present within the smectites.

Results of the extractions from both schemes A and B confirm that the majority (more than 80% of total As content) of the arsenic is associated with an operationally defined clay fraction, determined by other techniques here to be dominated by Mg-rich trioctahedral smectite. Only a small fraction of arsenic (<10% of total As) is associated with each of the operationally defined minor phases (i.e. amorphous silica, sulphides and Fe oxyhydroxides).

Only small amounts (<1% of total As) of operationally defined non-specifically sorbed arsenic were found by chemical extractions in any of the samples (Table 4). Furthermore, XPS surface chemical analysis aimed at detecting the concentration of arsenic on the mineral surfaces did not detect any peaks corresponding to Fe, S or As. Instead, the XPS spectra (data not shown) reflect the major element composition of the smectite (i.e. Si, Mg, Al, O). These observations, together with the need to apply a rigorous extraction (e.g. HCl-HNO_3 or HNO_3-HF) to release the bulk of the arsenic into solution strongly suggest that the arsenic is either predominantly dissolved within or occurring as sub-microscopic minerals occluded within the clay fraction, rather than being sorbed onto surfaces. However, it cannot be concluded definitively from these results alone that the trioctahedral smectite structurally incorporated arsenic based on the bulk selective extractions alone.

Arsenic coordination environments from XANES and EXAFS

The shape and position of the near edge (XANES) spectra of samples B-2 and C-6 (data not shown) are consistent with the majority of the arsenic being present as As(III)-O coordinated species. Modelling the XANES as a mixture of As(III)-O and As(V)-O coordinated species indicated that <10% of an As(V)-O coordinated species was present in sample B-2, and up to 30% of an As(V)-O coordinated species was present in sample C-6. The EXAFS spectra and associated Fourier transforms (Fig. 3), which give the approximate radial distributions of atoms around the central arsenic atoms, reveal, in addition to the peak due to As-O, the presence of additional surrounding atoms. This suggests the presence of an arsenic sulphide phase, which is consistent with the sparsely distributed sulphides observed under optical microscopy and the observation of a minor fraction of the total arsenic in these samples being associated with an operationally defined sulphide phase (Table 4). The best-fit average As−O bond length for sample B-2 is 1.73 Å while for C-6 it is 1.71 Å. Since a typical As(III)−O bond length is 1.79 Å and a typical As(V)−O bond length is 1.69 Å (Gault *et al.*, 2003, 2005 and references therein), this suggests the presence of As(V), in agreement with the XANES interpretation. An outer shell at ~3.4 Å could be fitted using Na, Fe (3.36−3.40 Å; Manning *et al.*, 1998), Al (3.16−3.51 Å; Arai *et*

TABLE 4. Arsenic in phases operationally defined by sequential selective chemical extractions. All concentrations expressed as mg kg^{-1}.

Sample	Scheme A			Scheme B		
	Sorbed	Silica-complexed	Clays	Fe-OH	Sulphides	Clay
B-2	16	150	2400	3.2	0	1500
C-6	49	510	4000	320	290	3500
CE-1	40	420	*n/m	250	350	2800
E-9	42	380	*n/m	320	400	3400

* n/m: not measured

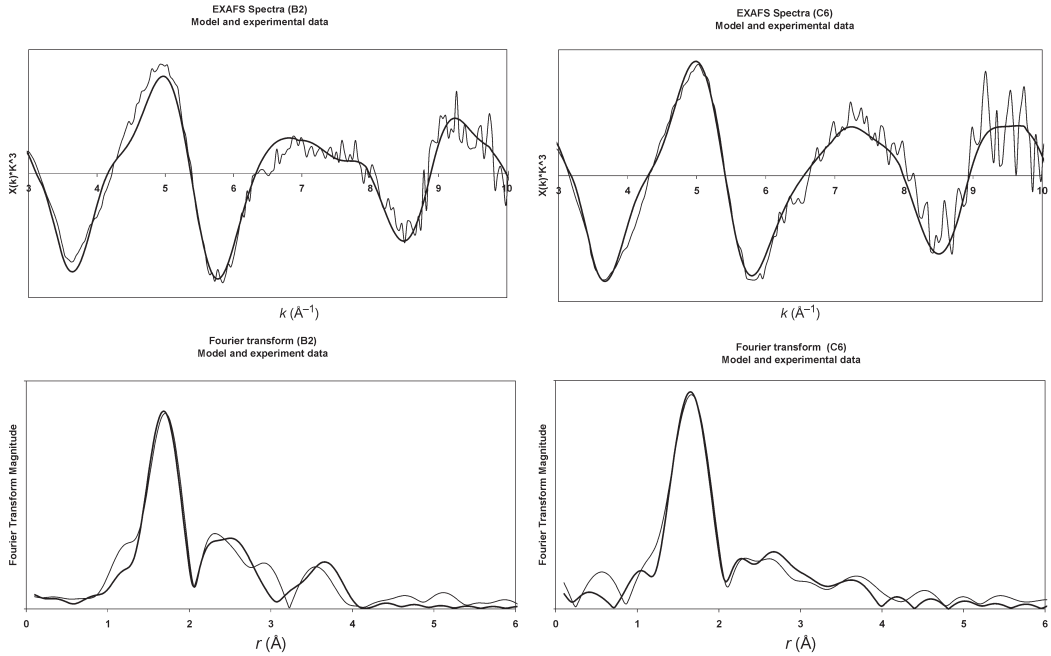

FIG. 3. Arsenic K-edge EXAFS spectra and Fourier transforms for geothermal scales B-2 and C-6. Bold lines indicate model data; fine lines indicate experimental data. The fits (see text) suggest the dominance of As(III)-O coordination environments with lesser contributions from As(V)-O coordination environments.

al., 2001) or As scatterers; it is not possible to discriminate significantly between these various possible scatterers.

Discussion

Arsenic hosts in the geothermal scales

Prior to this study, arsenic-bearing sulphides were predicted to contribute the largest amount of arsenic to the geothermal scales studied here. However, sulphide phases were sparsely observed in the samples via optical microscopy and were not detected by XRD, IR spectroscopy, or SEM-EDS chemical mapping. Results of the extractions are in agreement with these observations; sulphides are not the major contributor to the arsenic concentrations in the geothermal scales. Surface chemical analyses with XPS did not detect the Fe and S peaks that can be associated with either an arsenic-bearing sulphide mineral or Fe oxyhydroxides. Surface sorbed arsenic is almost negligible in amounts detected by XPS. The EXAFS results confirm that sulphide minerals are not the main source of arsenic in these samples, since As(III)-O-coordinated species are predominant. The minor amount of sulphide-associated arsenic species suggested by EXAFS is consistent with the minor amount of arsenic associated with operationally defined sulphide phases determined by the bulk selective chemical extractions performed, and the observations from optical microscopy.

We speculate that the non-sulphide-associated As(V)-O coordinated species found by XAS are possibly associated with the operationally defined amorphous silica phase since, of the two samples for which XAS data were obtained, the greater proportion (by a factor of ~3) of As(V)-O-coordinated species was found in sample C-6, which contains the greater proportion (by a factor of ~2) of arsenic associated with the operationally defined amorphous silica phase. The possible affinity of arsenic for incorporation into silicate structures is suggested by the occurrence of the arsenic silicate mineral filatovite (Vergasova *et al.*, 2004; Filatov *et al.*, 2004); however the possibility also exists that As(V) associated with this operationally defined phase occurs sorbed onto or within Fe oxyhydroxide occlusions. We also recognize that the possibility that As(V)-O-coordinated species may also occur within the smectites cannot be eliminated here.

The As K-edge XAS spectra represent the average of all the coordination environments analysed in the bulk samples, so it is difficult to quantify the amount of arsenic associated with each possible mineralogical host. The selective chemical extractions coupled with mineralogical characterizations suggest that the majority of the arsenic in these geothermal precipitates is associated with Mg-rich trioctahedral smectite (specifically in sample B-2). Qualitative micro-analyses with SEM-EDS detected arsenic in the smectite, and it is already shown that sulphides are not the major contributor to the arsenic concentrations found in the geothermal scales. These two lines of evidence suggest that the non-sulphide associated As(III)-O coordinated species detected by XAS is associated with As bound within the structure of the Mg-rich trioctahedral smectite. Trace metals such as Ni, Zn and Co have been reported previously to initially sorb on precursory phases later forming a trioctahedral smectite phase (Manceau *et al.*, 1985; Manceau and Calas, 1986; Charlet and Manceau, 1994; Manceau *et al.*, 1999; Dähn *et al.*, 2001). A similar mechanism could be responsible for the formation of the As-bearing smectites reported in this study.

Implications for the disposal of geothermal wastes and retrieval of useable materials

The bulk selective chemical extractions imply that any danger of arsenic being released into the surface environment is associated mostly with the dissolution of reducible phases and sulphide minerals. Although typically constituting <20% of the total arsenic in these geothermal precipitates, the contributions of arsenic from each of these operationally defined phases are substantial enough to be of a major concern for the geothermal wastes that are temporarily stored in the surface environment.

Previous studies have explored the retrieval of useable materials from the geothermal environment (e.g. Gallup *et al.*, 2003; Kato *et al.*, 2003) but have been beset by the accumulation of arsenic in the retrieved materials. The implied stability of arsenic in amorphous silica and smectites further hamper such efforts.

Conclusions

The risk of arsenic being released from geothermal scales depends largely on its mineralogical hosts; these hosts have been identified here in geothermal precipitates from a geothermal field in northern Japan by selective extractions, XRD, IR spectroscopy and SEM-EDS chemical analyses, whereas arsenic has been speciated by XAS. Dissolution of reducible phases (e.g. Fe oxyhydroxides) and sulphide minerals, albeit minor phases in the studied scales, could lead to the contamination of surface environments if the geothermal scales are not properly stored and disposed of. Furthermore, the retrieval of useable materials from the geothermal scales may be significantly and deleteriously impacted by the presence of arsenic within the clay mineral phases, notably smectite.

Although this is the first reported occurrence of an As(III)-bearing smectite, other trace metals have been reported as being incorporated in trioctahedral smectites; this suggests both the importance of understanding the mechanisms of arsenic uptake into the smectite structure and a possible, to be tested, application for the remediation of arsenic (or other trace metals) contaminated waters through uptake into trioctahedral smectites.

Acknowledgements

We are grateful for the following people who have helped in the analyses of the samples in this study: M. Takada and K. Ito (Kanazawa University), and Y. Yajima (National Institute for Materials Science) for the ICP-MS analyses; Prof. T. Watanabe and Dr. T. Oba for the use of the SEM-EDS facility in Joetsu University of Education (Niigata, Japan); Dr K. Hatta performed the XPS analyses (Japan International Center for Agricultural Research); access to the samples and the field site through Dr A. Ueda and Dr K. Kato (Central Research Institute – Mitsubishi Materials Corporation, Japan). Bob Bilsborrow and Andrew Gault are thanked for assistance in the collection of XAS data at CCLRC Daresbury under beamtime award 43/322 to Polya and Gault. This study has been partially funded by the 21st century COE program of Kanazawa University. Comments and suggestions by Dr Eva Valsami-Jones, Dr Javier Cuadros and an anonymous reviewer are also much appreciated.

References

Arai, Y., Elzinga, E.J. and Sparks, D.L. (2001) X-ray absorption spectroscopic investigation of arsenite

and arsenate adsorption at the aluminum oxide-water interface. *Journal of Colloid and Interface Science*, **235**, 80–88.

Ariki, K., Kato, H., Ueda, A. and Bamba, M. (2000) Characteristics and management of the Sumikawa geothermal reservoir, northeastern Japan. *Geothermics*, **29**, 171–189.

Arnorsson, S. (2003) Arsenic in surface- and up to 90ºC groundwaters in a basalt area, N-Iceland: processes controlling its mobility. *Applied Geochemistry*, **18**, 1297–1312.

Ballantyne, J. and Moore, J. (1988) Arsenic geochemistry in geothermal systems. *Geochimica et Cosmochimica Acta*, **52**, 475–483.

Charlet, L. and Manceau, A. (1994) Evidence for the formation of clays upon sorption of Co(II) and Ni(II) on silicates. *Geochimica et Cosmochimica Acta*, **58**, 2577–2582.

Criaud, A. and Fouillac, C. (1989) The distribution of arsenic (III) and arsenic (V) in geothermal waters: Examples from the Massif Central of France, the Island of Dominica in the Leeward Islands of the Caribbean, the Valles Caldera of New Mexico, U.S.A., and southwest Bulgaria. *Chemical Geology*, **76**, 259–269.

Dähn, R., Scheidegger, A.M., Manceau, A., Schlegel, M.L., Baeyens, B. and Bradbury, M.H. (2001) Ni clay neoformation on montmorillonite surface. *Journal of Synchrotron Radiation*, **8**, 533–535.

Ellis, A.J. (1977) Geothermal fluid chemistry and human health. *Geothermics*, **6**, 175–182.

Filatov, S.K., Krivovichev, S.V., Burns, P.C. and Vergasova, L.P. (2004) Crystal structure of filatovite, $K[(Al,Zn)_2(As,Si)_2O_8]$, the first arsenate of the feldspar group. *European Journal of Mineralogy*, **16**, 537–543.

Gallup, D.L., Sugiaman, F., Capuno, V. and Manceau, A. (2003) Laboratory investigation of silica removal from geothermal brines to control silica scaling and produce usable silicates. *Applied Geochemistry*, **18**, 1597–1612.

Gault, A.G., Polya, D.A., Charnock, J.M., Islam, F.S., Lloyd, J.R. and Chatterjee, D. (2003) Preliminary EXAFS studies of solid-phase speciation of As in a West Bengali sediment. *Mineralogical Magazine*, **67**, 1183–1191.

Gault, A.G., Cooke, D.R., Townsend, A.T., Charnock, J.M. and Polya, D.A. (2005) Mechanisms of arsenic attenuation in acid mine drainage from Mount Bischoff, western Tasmania. *Science of the Total Environment*, **345**, 219–228.

Ianni, C., Ruggieri, N., Rivaro, P. and Frache, R. (2001) Evaluation and comparison of two selective extraction procedures for heavy metal speciation in sediments. *Analytical Sciences*, **17**, 1273–1278.

Inoue, A., Utada, M. and Shimizu, M. (1999) Mineral-fluid interactions in the Sumikawa geothermal system, northeast Japan. *Resource Geology, Special Issue*, **20**, 79–97.

Inoue, T. and Ueda, R. (1965) On the Hanakawa fault, Akita, Japan. *Journal of the Mining College Akita University Serials A*, III, 15–29.

Kato, K., Ueda, A., Mogi, K., Nakazawa, H. and Shimizu, K. (2003) Silica recovery from Sumikawa and Ohnuma geothermal brines (Japan) by addition of CaO and cationic precipitants in a newly developed seed circulation device. *Geothermics*, **32**, 203–350.

Kumagai, N., Tanaka, T. and Kitao, K. (2004) Characterization of geothermal fluid flows at Sumikawa geothermal area, Japan, using two types of tracers and an improved multi-path model. *Geothermics*, **33**, 257–275.

Le Guern, C., Baranger, P., Crouzet, C., Bodenan, F. and Conil, P. (2003) Arsenic trapping by iron oxyhydroxides and carbonates at hydrothermal spring outlets. *Applied Geochemistry*, **18**, 1313–1323.

Manceau, A. and Calas, G. (1986) Ni-bearing clay minerals. 2. X-ray absorption study of Ni-Mg distribution. *Clay Minerals*, **21**, 341–360.

Manceau, A., Calas, G. and Decarreau, A. (1985) Nickel-bearing clay minerals. 1. Optical spectroscopic study of nickel crystal chemistry. *Clay Minerals*, **20**, 367–387.

Manceau, A., Schlegel, M., Nagy, K.L. and Charlet, L. (1999) Evidence for the formation of trioctahedral clay upon the sorption of Co^{2+} on quartz. *Journal of Colloid and Interface Science*, **220**, 181–197.

Manning, B.A., Fendorf, S.E. and Goldberg, S. (1998) Surface structure and stability of arsenic(III) on goethite: Spectroscopic evidence for inner-sphere complexes. *Environmental Science and Technology*, **32**, 2383–2388.

Okuma, S. (1998) Magnetic constraints on the subsurface structure of Akita-Yakeyama volcano, northeast Japan. *Earth, Planets and Space*, **50**, 153–163.

Peralta, G.L., Graydon, J.W. and Kirk, D.W. (1996) Physicochemical characteristics and leachability of scale and sludge from Bulalo geothermal system, Philippines. *Geothermics*, **25**, 17–35.

Polya, D.A., Lythgoe, P.R., Abou-Shakra, F., Gault, A.G., Brydie, J.R., Webster, J.G., Brown, K.L., Nimfopoulos, M.K. and Michailidis, K.M. (2003) IC-ICP-MS and IC-ICP-HEX-MS determination of arsenic speciation in surface and groundwaters: preservation and analytical issues. *Mineralogical Magazine*, **67**, 247–261.

Pritchett, J.W., Garg, S.K., Maki, H. and Kubota, Y. (1989) Hydrology of the Sumikawa geothermal prospect, Japan. *Energy Sources*, **11**, 251–262.

Rowland, H.A.L., Gault, A.G., Charnock, J.M. and Polya, D.A. (2005) Preservation and XANES

determination of the oxidation state of solid phase arsenic species in shallow sedimentary aquifers in Bengal and Cambodia. *Mineralogical Magazine*, **69**, 825–839.

Sakai, Y., Kubota, Y. and Hatakeyama, K. (1986) Geothermal exploration at Sumikawa, north Hachimantai, Akita. *Chinetsu*, **23**, 281–302.

Smedley, P.L. and Kinniburgh, D.G. (2002) A review of the source, behaviour and distribution of arsenic in natural waters. *Applied Geochemistry*, **17**, 517–568.

Tessier, A., Campbell, P.G.C. and Bisson, M. (1979) Sequential extraction procedure for speciation of particulate trace metals. *Analytical Chemistry*, **51**, 844–851.

Ueda, A., Kubota, Y., Katoh, H., Hatakeyama, K. and Matsubaya, O. (1991) Geochemical characteristics of the Sumikawa geothermal system, northeast Japan. *Geochemical Journal*, **25**, 223–244.

Velde, B. (1992) *Introduction to Clay Minerals: Chemistry, Origin, Uses and Environmental Significance*. Chapman & Hall, London, 198 pp.

Vergasova, L.P., Krivovichev, S.V., Britvin, S.N., Burns, P.C. and Ananiev, V.V. (2004) Filatovite, $K[(Al,Zn)_2(As,Si)_2O_8]$, a new mineral species from the Tolbachik volcano, Kamchatka peninsula, Russia. *European Journal of Mineralogy*, **16**, 533–536.

Yora, M., Wakita, K. and Honda, S. (1973) Exploration of Onuma geothermal field, Northeastern Japan. *Chinetsu*, **10**, 27–44.

[*Manuscript received 27 January 2005: revised 26 July 2005*]